



CHALMERS
UNIVERSITY OF TECHNOLOGY

Probing molecular orientation of donors and acceptors in all-polymer blend films by near-edge x-ray absorption fine structure spectroscopy

Downloaded from: <https://research.chalmers.se>, 2026-03-03 19:45 UTC

Citation for the original published paper (version of record):

Christopholi, L., Wolkeba, Z., Marchiori, C. et al (2026). Probing molecular orientation of donors and acceptors in all-polymer blend films by near-edge x-ray absorption fine structure spectroscopy. *JPhys Materials*, 9(2).
<http://dx.doi.org/10.1088/2515-7639/ae409d>

N.B. When citing this work, cite the original published paper.

PAPER • OPEN ACCESS

Probing molecular orientation of donors and acceptors in all-polymer blend films by near-edge x-ray absorption fine structure spectroscopy

To cite this article: Leticia P Christopholi *et al* 2026 *J. Phys. Mater.* **9** 025001

View the [article online](#) for updates and enhancements.

You may also like

- [When adiabaticity is not enough to study topological phases in solid-state physics: comparing the Berry and Aharonov–Anandan phases in 2D materials](#)

Abdiel de Jesús Espinosa-Champo, Alejandro Kunold and Gerardo G Naumis

- [Recent advances in conducting polymer chemiresistive sensors for ammonia gas detection: materials, characterization, and applications](#)

Annelot Nijkoops, Manuela Ciocca, Martina Aurora Costa Angeli *et al.*

- [The 2025 roadmap to ultrafast dynamics: frontiers of theoretical and computational modeling](#)

Fabio Caruso, Michael A Sentef, Claudio Attaccalite *et al.*



PAPER

OPEN ACCESS

RECEIVED
3 September 2025REVISED
23 December 2025ACCEPTED FOR PUBLICATION
2 February 2026PUBLISHED
16 February 2026

Original content from this work may be used under the terms of the [Creative Commons Attribution 4.0 licence](#).

Any further distribution of this work must maintain attribution to the author(s) and the title of the work, journal citation and DOI.



Probing molecular orientation of donors and acceptors in all-polymer blend films by near-edge x-ray absorption fine structure spectroscopy

Leticia P Christopholi¹ , Zewdneh Genene² , Cleber F N Marchiori¹ , Stela Andrea Muntean¹ , Ergang Wang² and Ellen Moons^{1,*} ¹ Department of Engineering and Physics, Karlstad University, SE-65188 Karlstad, Sweden² Department of Chemistry and Chemical Engineering, Chalmers University of Technology, SE-412 96 Göteborg, Sweden

* Author to whom any correspondence should be addressed.

E-mail: ellen.moons@kau.se**Keywords:** NEXAFS, molecular orientation, all-polymer blend, organic photovoltaicsSupplementary material for this article is available [online](#)

Abstract

The molecular orientation is crucial for the efficiency of organic solar cells. A face-on orientation, in which the $\pi - \pi$ stacking direction is oriented perpendicular to the substrate, is typically preferred because it enhances vertical charge transport to the electrodes and can additionally modify the position of energy levels. In this study, near-edge x-ray absorption fine structure (NEXAFS) spectroscopy was employed to investigate the molecular orientation of the acceptor polymers PYT and PF5-Y5 and the donor polymer PBDB-T in spin-coated blend films with different donor: acceptor ratios. From the comparison of NEXAFS spectra acquired in partial electron yield (PEY), total electron yield (TEY), and fluorescence yield (FY) modes, depth-dependent information about the orientation of the components in the films can be extracted. We found that the absorption resonances in the PEY carbon K-edge spectra of all the blend films resembled the spectral signatures of PBDB-T, indicating that the surface of these blend films is PBDB-T-rich, even at a 1:10 donor-to-acceptor ratio. To identify the acceptor component in the carbon spectra, deeper subsurface probing was required using TEY and FY modes, alongside analysis of the angular dependence of these spectra. Nitrogen K-edge NEXAFS spectra were employed to selectively probe the acceptor orientation in the blend films, revealing that generally the polymer acceptors retain their face-on orientation observed in neat acceptor films. However, in one blend, a decrease in the dichroic ratio suggests that the donor polymer influences the molecular orientation of the acceptor at the film's surface. This work demonstrates a novel strategy to probe molecular orientation in all-polymer blend films. The approach exploits dichroism at selective absorption edges to access detailed information on the molecular orientation of one component within the blend film.

1. Introduction

Recent advancements in new organic semiconductors have enabled organic solar cells (OSCs) to achieve record-breaking power conversion efficiencies (PCEs) exceeding 19% [1–4]. Typically, the photoactive layer in OSCs is processed from a blend solution of electron donor and electron acceptor molecules, forming a nanoscale network known as the bulk heterojunction. The performance enhancement is primarily attributed to the development of non-fullerene acceptors (NFAs) also referred to as small molecules (SMAs). Among these, the so-called Y-series of SMAs—characterized by planar ADA'DA architecture, where A and A' are electron-withdrawing units and D is an electron-donating unit—have played a key role [5]. Despite their promising efficiency, OSCs based on small molecule NFAs exhibit low thermal and mechanical stability, posing a significant obstacle to the commercialization of OSCs. To overcome these limitations, the polymerization of SMAs has emerged as a promising strategy [6]. Studies

reveal that alternating copolymer structure, significantly enhances material properties. For example, SMA-based polymer acceptors improve mechanical robustness and thermal stability, with all-polymer blends retaining over 90% of their initial PCE after prolonged heating at 100 °C [7, 8]. These improvements highlight the potential of polymer acceptors for more durable and efficient OPVs. Additionally, molecular factors such as backbone planarity, interchain packing, and molecular orientation remain critical for device performance in all-polymer solar cell [9–12].

Specifically, regarding molecular orientation, studies have shown that in NFA-based OSCs, it strongly influences charge mobility and interfacial energetics by governing $\pi - \pi$ stacking and orbital overlap between conjugated backbones. Zhou *et al* [13] used bilayer devices to investigate the effect of molecular orientation on open-circuit voltage (V_{OC}). They found that the polymer acceptor's orientation primarily drives V_{OC} loss in all-polymer solar cells. Lee *et al* [14] found enhanced exciton diffusion for face-on oriented active layers due to reduced geminate recombination of charge pairs, resulting in enhanced photocurrent generation. Zhou *et al* [15] showed that a correlated donor/acceptor face-on/face-on molecular orientation enhances hole and electron mobilities by a factor 6. In addition, Li *et al* [16] mapped the energy level alignment at donor/acceptor interfaces and demonstrated that molecular orientation directly shifts interfacial energy levels.

Morphology studies on polymer films, including those mentioned above, frequently rely on grazing incidence wide-angle x-ray scattering (GIWAXS). While this is a versatile technique for examining the molecular aggregation, molecular packing and crystallinity in thin films, GIWAXS is less suitable for studying molecular orientation. In contrast, near-edge x-ray absorption fine structure (NEXAFS) spectroscopy probes the molecular orientation of both crystalline and non-crystalline domains, while also providing information on the electronic structure. In our previous work we employed angular-dependent NEXAFS spectroscopy to investigate the effect of processing solvent on the molecular orientation of Y-type SMAs [17]. Beyond the commonly studied carbon K-edge, we also explored the nitrogen K-edge and assigned the relevant absorption transitions demonstrating the potential of this technique for materials characterization. Thanks to its chemical specificity, NEXAFS enables the selective investigation of individual components in blend films, if they exhibit distinct absorption resonances. This is particularly advantageous for organic molecules containing heteroatoms, where element-specific absorption edges can be used to distinguish the molecular orientation of donor and acceptor components within complex blends.

In this study, we employ NEXAFS spectroscopy to investigate the molecular orientation and electronic structure of films of two polymer acceptors, the Y5-based copolymers PYT and PF5-Y5, as well as their blends with PBDB-T in two different ratios, 1:0.75 and 1:10. These specific ratios were intentionally selected to explore the influence of blend composition on material properties. By comparing spectra obtained in the three different detection modes, partial electron yield (PEY), total electron yield (TEY), and fluorescence yield (FY), we gain insights into the distribution of the polymer donor and acceptors at different depths within the blend films. PEY provides the most surface-sensitive signal (≈ 1 nm), followed by TEY (≈ 3 nm), while FY offers bulk-sensitive information [18]. We find that, in contrast to our previous findings on SMA Y5 and Y6, which exhibited no preferential molecular orientation when processed from chlorobenzene (CB) solutions [17], the polymer films studied here display a clear face-on orientation under the same processing conditions. Furthermore, we demonstrate that the chemical selectivity of NEXAFS enables the investigation of the mutual influence of donor and acceptor components on the molecular orientations in the blend films. For these blend systems, where the polymer acceptors contain nitrogen atoms, while the donor PBDB-T does not, the nitrogen K-edge spectra serve as a distinct fingerprint of the acceptor, providing direct information about the molecular orientation of the acceptor in the blend. Using the dichroic ratio, we compare the degree of orientation of the acceptor in the blend films with that in the neat acceptor films. This level of chemical selectivity is not achievable in the carbon K-edge spectra due to the predominantly overlapping x-ray absorption resonances of donor and acceptor molecules.

2. Method

The polymer acceptors PYT and PF5-Y5 consist of alternating electron-deficient Y5 units and donor moieties, i.e. thiophene and thienyl-benzodithiophene (BDT-T), respectively. The synthesis of PYT ($M_w = 27.2$ kDa, PDI ≈ 2.6) and PF5-Y5 ($M_w = 9.8$ kDa, PDI = 1.93) are described in detail in previous publications [19, 20]. The polymer donor PBDB-T (poly[[4,8-bis[5-(2-ethylhexyl)-2-thienyl]benzo[1,2-b:4,5-b']dithiophene-2,6-diyl]-2,5-thiophenediyl[5,7-bis(2-ethylhexyl)-4,8-dioxo-4 H,8 H-benzo[1,2-c:4,5-c']dithiophene-1,3-diyl]]) ($M_w = 65$ kDa, PDI = 2.3) was purchased from 1-Material (Canada). CB (analytical grade) was purchased from Sigma-Aldrich. Stock solutions of donor

and acceptor polymers in CB were prepared with a concentration of 7 mg ml⁻¹. The solutions were stirred overnight while heated at 100 °C. Donor-only, acceptor-only, and donor:acceptor blend thin films with volume ratios 1:0.75 and 1:10 were spin-coated at 2000 rpm for 60 s on silicon substrates. The silicon substrates were cleaned before deposition using the RCA method without the final hydrofluoric acid etching step [21]. The thin films were prepared in a nitrogen-filled glovebox under yellow light.

Morphology and thickness measurements were carried out using a Nanoscope 8 Multimode AFM (Bruker, France) in tapping mode with silicon tip (model: RTESPA-300, Bruker). For thickness measurements the tip was moved across a scratch that was intentionally made in the film.

The polymer films on silicon substrates were investigated by NEXAFS spectroscopy at carbon K-edge and nitrogen K-edge, performed at the FlexPES beamline at the Swedish National Laboratory MAX IV in Lund, Sweden. The samples were transported to the synchrotron in air-tight bags filled with N₂ and kept in the dark until they were mounted on the sample holders and inserted in the UHV system; to minimize time they were exposed to air and light. The x-ray source at the FlexPES beamline is a linearly polarizing undulator U54.4, providing horizontally polarized radiation in the 40 eV–1500 eV range.

NEXAFS is a powerful technique for probing the orientation of the conjugated plane in these polymers, as the transition dipole moment associated with the excitation of a core electron to the unoccupied states is directionally specific in aromatic systems [22, 23]. To investigate the angular dependence of the x-ray absorption for specific resonances, NEXAFS spectra were recorded at five different angles of incidence: 90°, 70°, 55°, 40°, and 30°, with respect to the sample surface. Each angular series was terminated with a repetition of the measurement at 90°, to check for the presence of beam-induced damage. Measurements were performed on a fresh spot for each absorption edge.

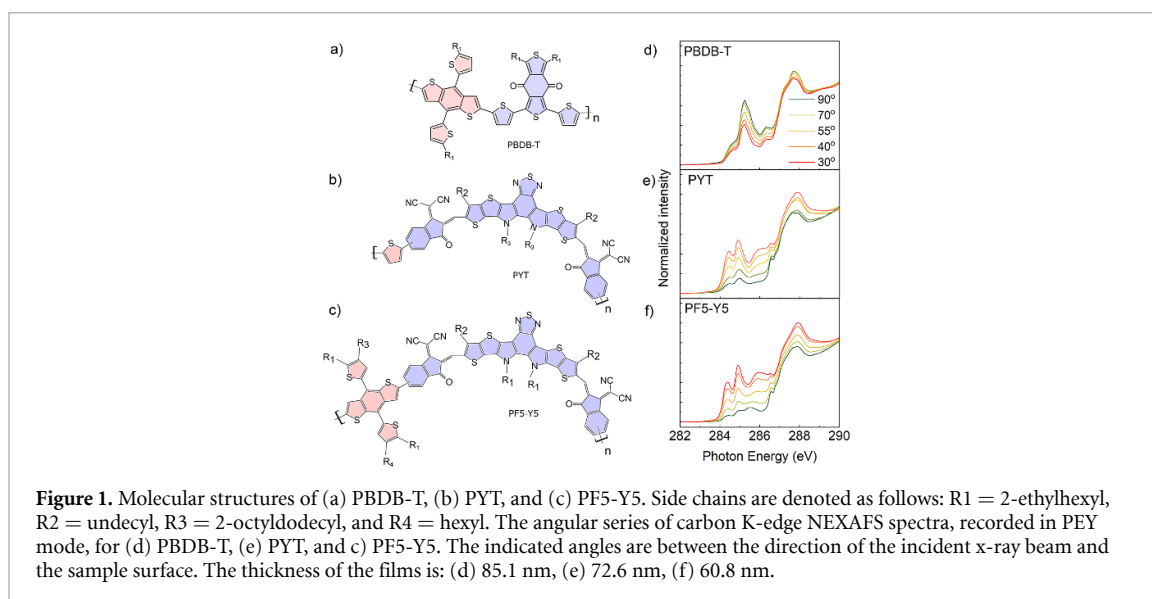
NEXAFS spectra in PEY mode were recorded by detecting emitted electrons with a MCP detector using a retardation voltage of 150 V for the carbon and nitrogen absorption edges. NEXAFS spectra in partial FY mode were acquired by detecting the emitted photons using a Sirius SDD with a 70 mm² active area (Rayspec), coupled with an Xspress3mini pulse processor (Quantum Detectors). Data analysis was performed with PyMca 5.6.7 [24]. The spectral data were normalized by subtracting a linear baseline (considering both slope and offset) in the pre-edge region and setting the post-edge intensity to unity for each absorption edge. For the carbon K-edge, the pre-edge range was 270 eV–282 eV and the post-edge at 320 eV–340 eV. For the nitrogen K-edge, the pre-edge range was 390 eV–397 eV and the post-edge at 410 eV–425 eV. The angular dependence of the intensities of the absorption resonances is quantified by the dichroic ratio, given by $D = \frac{I_{90^\circ} - I_{30^\circ}}{I_{90^\circ} + I_{30^\circ}}$, where I_{90° is the absorption intensity at perpendicular incidence and I_{30° is the absorption intensity at near-grazing incidence for a selected resonance. The dichroic ratio ranges from -1 to 1, where 1 indicates perfect edge-on orientation, 0 indicates no preferential orientation, and -1 indicates perfect face-on orientation.

3. Results and discussion

The molecular structures of the polymer donor PBDB-T and the polymer acceptors PYT and PF5-Y5 are shown in The chemical structure of PBDB-T (figure 1(a)) consists of two building blocks: a donor unit, 2-alkylthiophene-substituted benzo[1,2-b:4,5-b']dithiophene (BDT), marked in pink, and an acceptor unit, 1,3-bis(thiophen-2-yl)-5,7-bis(2-ethylhexyl)benzo-[1,2-c:4,5-c']dithiophene-4,8-dione (BDD), in purple [25]. The acceptor polymers, PYT (figure 1(b)) and PF5-Y5 (figure 1(c)), are alternating copolymers based on the small molecule Y5 as one of the moieties. PYT features an alternating structure of Y5 acceptor units (purple) and thiophene donor units (pink). In contrast, PF5-Y5 comprises alternating Y5 acceptor units (purple) and BDT-T donor moieties (pink).

Figures 1(d)–(f) present the angle-dependent carbon K-edge NEXAFS spectra, recorded in PEY mode, for pure PBDB-T, PYT, and PF5-Y5 films, respectively. The PBDB-T spectra show a weak dichroism of the carbon 1s → π* absorption resonances at ~ 284.5 eV and ~ 285.3 eV. A decrease in absorption intensity with decreasing incidence angle (θ) from 90° (normal incidence) to 30° (grazing incidence) indicates a weak preferential edge-on orientation of the conjugated plane of PBDB-T.

The PYT and PF5-Y5 spectra exhibit pronounced dichroism of the carbon 1s → π* absorption resonances at ~ 284.3 eV and ~ 284.9 eV. For both materials, the absorption intensity increases as the incidence angle decreases from normal to grazing incidence, indicating a preferential face-on orientation of the conjugated backbones. The peaks related to the carbon 1s → π* transitions can be identified in the range of ~ 283 eV–289.5 eV, followed by σ* resonances above ~ 289.5 eV up to 314 eV, where the EXAFS region starts, considering an ionization threshold about 30 eV from the near edge region (full range spectra are included in the supporting information) [26]. These σ* resonances arise from multiple molecular components, including both the conjugated backbone and the side chains. The resonances associated with the conjugated plane are expected to exhibit an opposite angular dependence



compared to the π^* transition. However, contributions from side chains may present a different angular behavior, as they are not necessarily aligned in the same way. Therefore, the observed angular dependence in this region likely reflects a combination of these distinct contributions.

The carbon $1s \rightarrow \pi^*$ transition peaks, along with other spectral features, closely resemble those observed in NEXAFS spectra of Y5 films [17]. According to TD-DFT calculations presented in [17], the first two peaks at ~ 284.34 eV and ~ 284.77 eV in the Y5 carbon K-edge spectrum originate from electronic excitations from core levels in specific carbon atoms located within the fused-ring structures of the acceptor moieties and at the bridge connecting the donor and acceptor moieties. The π^* -type final states of these transitions are delocalized over the conjugated backbone.

Since NEXAFS probes the transition probability from the core level to unoccupied molecular orbitals, the observed spectral features are directly related to the density of states of the lowest unoccupied molecular orbitals (LUMO) and higher unoccupied molecular orbitals. The strong similarity in spectral features indicates that the NEXAFS spectra of the acceptor polymers PYT and PF5-Y5 are dominated by the transitions associated with the Y5 co-mer. This behavior is consistent with the nature of donor-acceptor copolymers, where in a ‘weak donor–strong acceptor’ configuration, the donor moiety typically contributes to the highest occupied molecular orbitals, while the acceptor moiety defines the LUMO of the resulting copolymer [27].

Figure 2 shows the carbon K-edge spectra, recorded in PEY mode, for the blends PBDB-T:PYT and PBDB-T:PF5-Y5 with ratios 1:0.75 and 1:10. When comparing the spectra of the 1:0.75 blends to those of pure PBDB-T and the corresponding pure acceptors (see figures 1(d)–(f)), it is evident that the absorption resonances in the blends’ spectra closely resemble those of PBDB-T – both in position and intensity. This suggests that, at the surface of the blend films, the spectral signature is dominated by the donor polymer. Interestingly, even in the 1:10 blends, where the acceptor content is then ten times higher, the carbon K-edge spectra still predominantly resemble that of PBDB-T.

To understand the orientation of the polymer backbones in these films, the degree of dichroism can be quantified from the angular dependence of the π^* resonances observed in the NEXAFS spectra. The maximum and the minimum absorption intensities, corresponding to the electric field vector being perpendicular and (almost) parallel to the backbone axis, respectively, are used to calculate the dichroic ratio [28]. In the present study, due to the experimental geometry, the minimum angle of measurement is 30° rather than 0° , which limits the direct measurement of the perfect face-on orientation. The dichroic ratio is thus determined from the observed absorption intensities at 30° and 90° .

Figures 3 and S1 summarize the dichroic ratios extracted from the π^* resonance at ~ 285 eV in the carbon K-edge and at ~ 398 eV in the nitrogen K-edge spectra for all samples across the different detection modes. The figure provides a comparative overview of the preferred molecular orientation as a function of composition of each of the films, visualizing differences between surface and bulk regions, as well as between neat and blended systems. We will first discuss the carbon K-edge before returning to the nitrogen K-edge.

Figure 3(a) shows the dichroic ratios for PBDB-T, PBDB-T:PYT (1:0.75), PBDB-T:PYT (1:10), and PYT. For the most surface sensitive mode (PEY) the extracted values are 0.22, 0.21, 0.09, and -0.57 ,

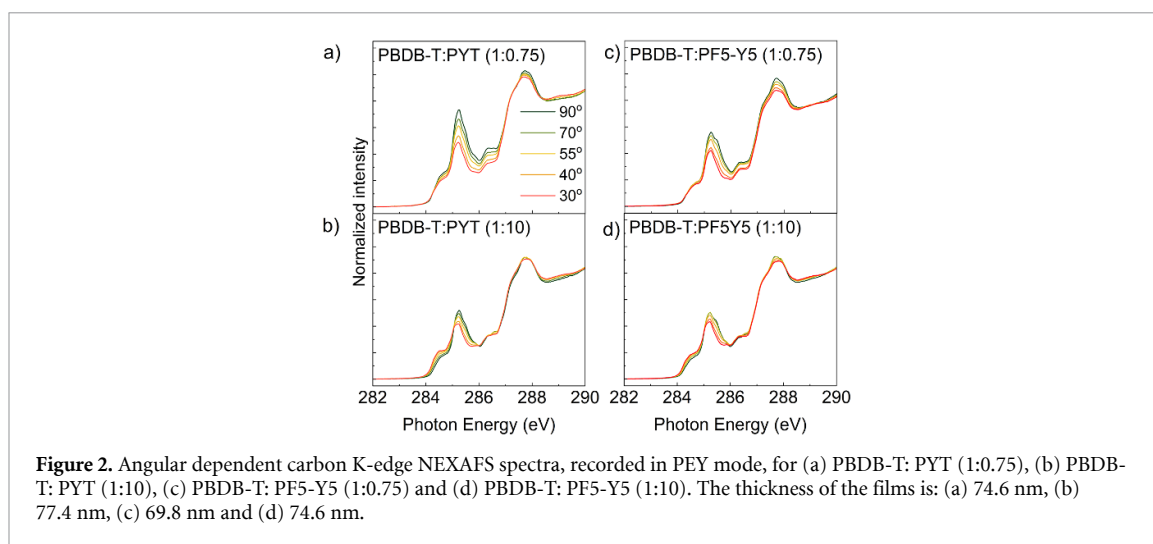


Figure 2. Angular dependent carbon K-edge NEXAFS spectra, recorded in PEY mode, for (a) PBDB-T:PYT (1:0.75), (b) PBDB-T:PYT (1:10), (c) PBDB-T:PF5-Y5 (1:0.75) and (d) PBDB-T:PF5-Y5 (1:10). The thickness of the films is: (a) 74.6 nm, (b) 77.4 nm, (c) 69.8 nm and (d) 74.6 nm.

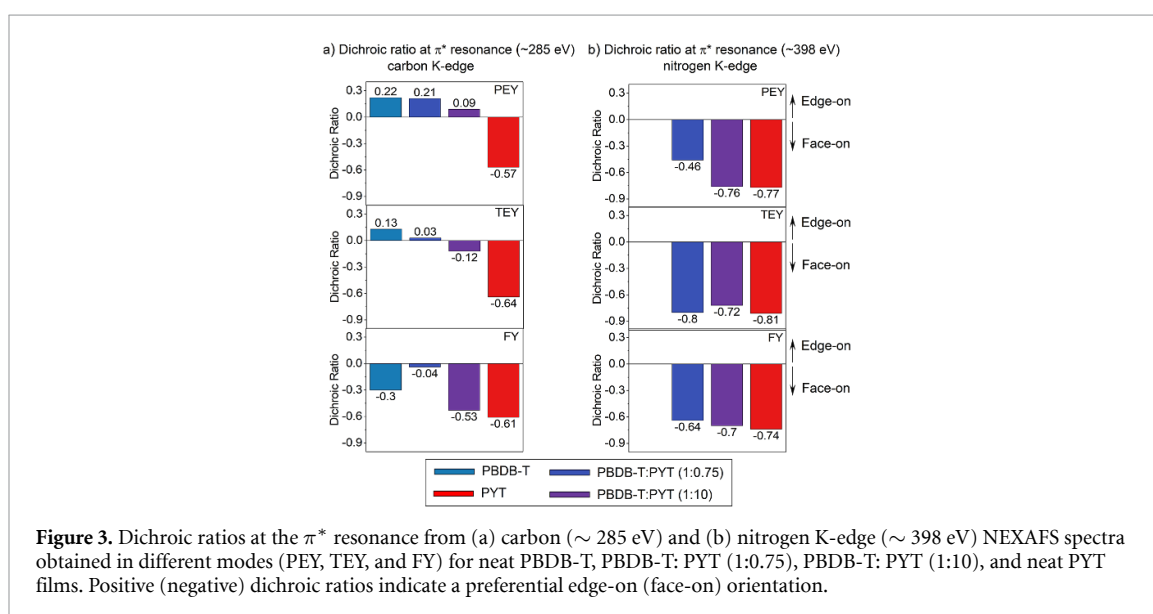
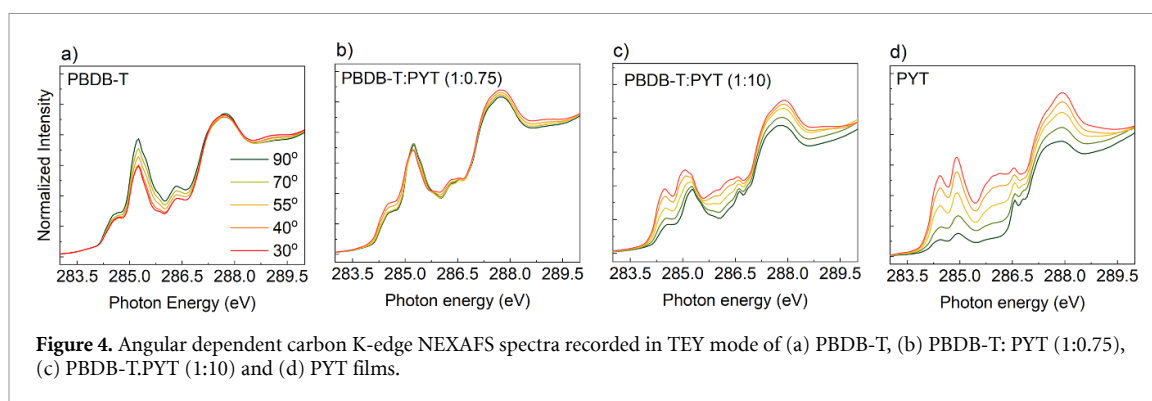


Figure 3. Dichroic ratios at the π^* resonance from (a) carbon (~ 285 eV) and (b) nitrogen K-edge (~ 398 eV) NEXAFS spectra obtained in different modes (PEY, TEY, and FY) for neat PBDB-T, PBDB-T:PYT (1:0.75), PBDB-T:PYT (1:10), and neat PYT films. Positive (negative) dichroic ratios indicate a preferential edge-on (face-on) orientation.

respectively. Figure S1(a) shows the corresponding dichroic ratios for PBDB-T (repeated for reference), PBDB-T:PF5-Y5 (1:0.75), PBDB-T:PF5-Y5 (1:10), and PF5-Y5. For the PEY mode the values are 0.22, 0.14, 0.07, and -0.64 . The positive dichroic ratios observed for PBDB-T indicate a weak preferential edge-on orientation of the conjugated backbone at the surface. In contrast, the pure acceptor films (PYT and PF5-Y5) exhibit strong face-on alignment, as evidenced by the large negative values derived from the carbon signal. For PBDB-T:PYT blends, a reduction in dichroic ratio is observed at high acceptor content, relative to that of pure PBDB-T. Conversely, PBDB-T:PF5-Y5 blends show a decrease in dichroic ratio even at low acceptor content, with further reduction at higher concentrations.

PEY mode is very surface-sensitive—probing only the top few nanometers of the film. To investigate the molecular orientation at the subsurface of the films, we employed TEY measurements. Figure 4 shows the carbon K-edge NEXAFS spectra recorded in TEY mode for neat PBDB-T and PYT films, as well as for the PBDB-T:PYT blend films with ratios of 1:0.75 and 1:10. The dichroic ratios extracted from these spectra are presented in figure 3(a)

As shown in figure 3(a), the dichroic ratio of PBDB-T films, extracted from the carbon K-edge spectra recorded in TEY mode are smaller (0.13) than those from PEY mode spectra (0.22). For the PBDB-T:PYT (1:0.75) blend, (figure 4(b)), the spectral shape at the carbon K-edge resembles that of the donor PBDB-T and shows practically no dichroism. In contrast, for the blend (1:10) (figure 4(c)), signals from the acceptor become more prominent when probing deeper into the film. In these TEY spectra of the (1:10) blend the spectral shape changes with angle. The peaks at ~ 284.5 eV and ~ 285.3 eV, which can be distinguished for the incidence angle $\theta = 90^\circ$, correspond to the PBDB-T carbon $1s \rightarrow \pi^*$ absorption resonances. As the incident angle decreases from 90° to 30° , these peaks gradually shift and resolve into



the first two carbon $1s \rightarrow \pi^*$ absorption resonances of the acceptor PYT at ~ 284.3 eV and ~ 284.9 eV. The small changes in peak intensity under angle variation (dichroic ratio: -0.12) indicate a slight preference for a face-on orientation in the sub-surface region of the film, likely reflecting the orientation of PYT in this blend film.

However, the observed spectral features near the carbon K-edge are influenced by the overlap of x-ray absorption resonances from both components in the blend film, which accounts for the lower dichroic ratio (-0.13) compared to the pure PYT film (-0.64). The more negative dichroic ratio observed for PYT in TEY mode (-0.64) relative to PEY mode (-0.57), indicates a stronger degree of face-on molecular orientation further away from the surface.

Figures S2(a)–(d) shows the angular dependent carbon K-edge spectra recorded in TEY mode for PBDB-T (repeated for reference), PBDB-T:PF5-Y5 (1:0.75), PBDB-T:PF5-Y5 (1:10), and PF5-Y5. The dichroic ratios for these films are 0.13, 0.09, -0.13 , and -0.60 for PBDB-T, PBDB-T:PF5:Y5 (1:0.75), PBDB-T:PF5-Y5 (1:10), and PF5-Y5, respectively, as shown in figure S1.

Together, these results show a consistent trend: the acceptor signature is nearly absent in the 1:0.75 blend—both in terms of spectral features and dichroism—and becomes distinguishable in the 1:10 blends mainly through the angular-dependence of the TEY spectra. This highlights the importance of both deeper angular-dependent and subsurface-sensitive probing for identifying the acceptor contributions, even if its content is increased ten-fold.

Notably, for the 1:0.75 blends no distinct spectral features of the acceptors can be identified in the carbon K-edge spectra in PEY and TEY mode. Furthermore, for the 1:10 blends, spectral features of the acceptor are observable only in TEY mode under angular variation. As result, it is not possible to determine whether the acceptors retain their orientation when blended with the donor PBDB-T. To overcome this limitation, an element that is specific to the acceptor, namely nitrogen, was used as a selective probe.

The orientation of the acceptor molecules in these blend films can be effectively characterized using nitrogen K-edge NEXAFS spectra, because the donor PBDB-T does not contain nitrogen in its composition (figure 1(a))

Figures S3(a)–(c) and 5(a)–(c) show the nitrogen K-edge NEXAFS spectra measured in PEY and TEY mode for PBDB-T:PYT (1:0.75), PBDB-T:PYT (1:10), and PYT, respectively. Decreasing the incidence angle, θ , of x-rays from 90° to 30° with respect to the surface leads to increased absorption intensity of the resonances at ~ 398.56 eV and ~ 400.9 eV, while the peak at ~ 399.55 eV exhibits the opposite angular dependence. The contributing transitions to the respective peaks in the nitrogen K-edge correspond to $1s \rightarrow \pi^*$ resonances from the two π -systems in the acceptor unit of PYT: the aromatic system (including the benzothiadiazole and the pyrrole) and the cyano triple bond system. These contributions explain the weaker or opposite angular dependence of the middle peak at ~ 399.55 eV, compared to that of the other two resonances, as detailed for Y5 and Y6 in [17].

The first $1s \rightarrow \pi^*$ resonance at ~ 398.56 eV, associated with orbitals perpendicular to the aromatic system, provides a clear indicator of molecular orientation. The pronounced increase in the intensity of the peak at grazing incidence confirms that the conjugated plane of PYT is face-on oriented both at the surface and in the subsurface region of the film, with dichroic ratio of -0.77 (PEY) and -0.81 (TEY) (figure 3(b)), consistent with the conclusions drawn from the carbon K-edge spectra. Furthermore, the nitrogen K-edge spectra confirm that PYT retains its orientation when blended with PBDB-T. The 1:0.75 and 1:10 blends exhibit dichroic ratios of -0.46 (PEY) and -0.80 (TEY), and -0.76 (PEY) and -0.72 (TEY), respectively, indicating a preserved face-on molecular orientation of the acceptor across both blend ratios. However, in the case of the PBDB-T:PYT (1:0.75) blend, the dichroic ratio for the PEY

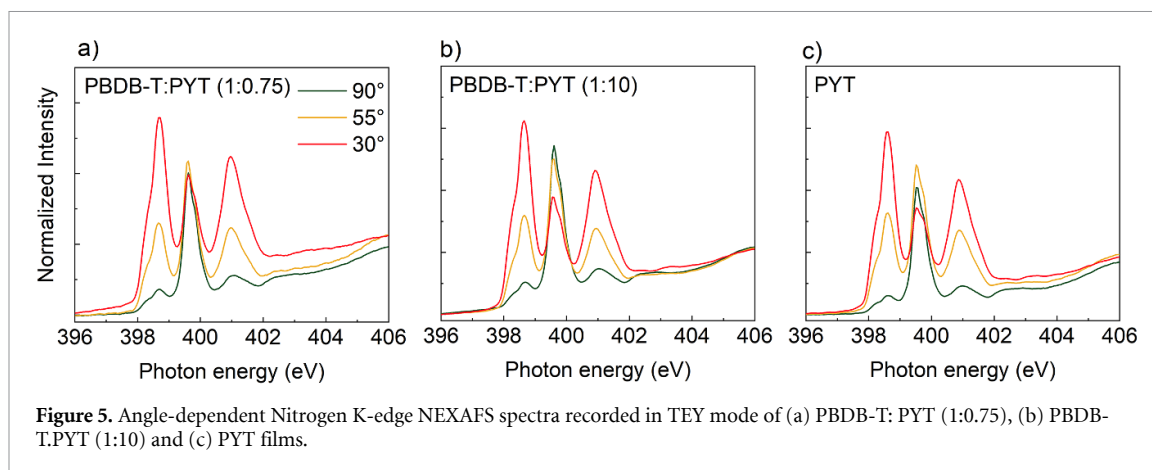


Figure 5. Angle-dependent Nitrogen K-edge NEXAFS spectra recorded in TEY mode of (a) PBDB-T:PYT (1:0.75), (b) PBDB-T:PYT (1:10) and (c) PYT films.

spectrum is significantly lower (-0.43) compared to that of the neat PYT (-0.77). This indicates that, on average, PYT is less face-on oriented at the surface of the PBDB-T:PYT (1:0.75) blend film, suggesting that PBDB-T affects the alignment of PYT at the film's surface.

The nitrogen K-edge spectra measured in PEY and TEY mode for PF5-Y5 and PBDB-T:PF5:Y5 blends are shown in figures S3(d)–(f) and S4(a)–(c). The dichroic ratios for neat PF5-Y5 calculated at π^* resonance at ~ 398.56 eV (seen in figure S1), are -0.74 (PEY) and -0.69 (TEY). This is consistent with the results from the carbon K-edge spectra confirming the face-on orientation of PF5-Y5 at the surface and in the subsurface region of the film. Moreover, the 1:0.75 and 1:10 blends exhibit dichroic ratios of -0.60 (PEY) and -0.74 (TEY), -0.66 (PEY) and -0.6 (TEY), indicating that PF5-Y5 retains its face-on orientation when blended with PBDB-T.

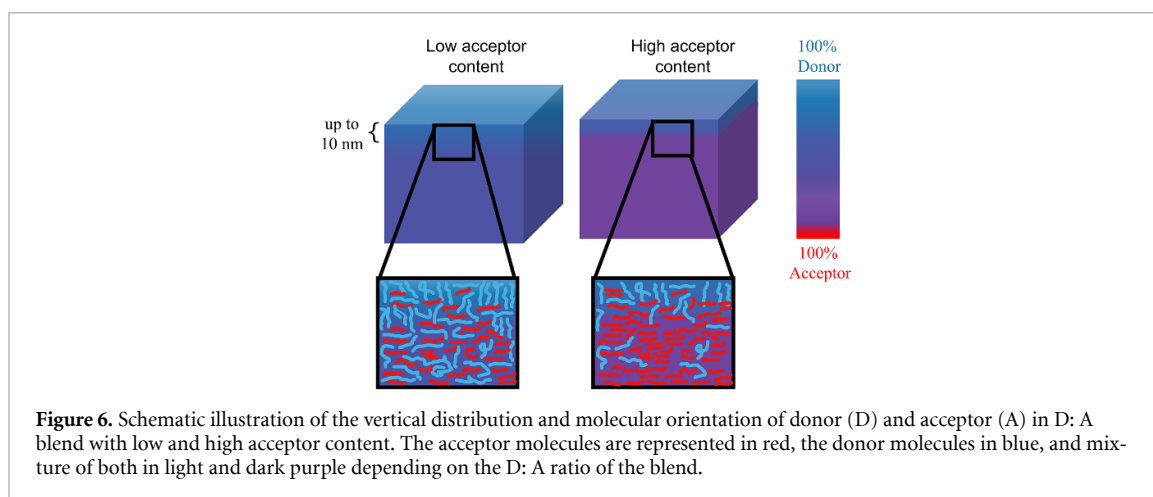
Finally, to get insights into the molecular orientation within the bulk film, we performed NEXAFS measurements in FY mode. Figure S5 shows the angular-dependent carbon K-edge NEXAFS spectra recorded in FY mode for PBDB-T, PYT, PF5-Y5, and their respective blends. Interestingly, in FY mode, PBDB-T exhibits a face-on orientation in the bulk with a dichroic ratio of -0.3 , in contrast to the slight tendency for edge-on orientation observed in the more surface-sensitive PEY and TEY modes. This is in agreement with the observations reported by Neusser *et al* [29] for PBDB-TF (PM6) films, spin-coated from chloroform (CF):chloro-naphthalene (CN) (0.5 wt%) mixtures. The authors showed by NEXAFS that PM6 has an average edge-on orientation at the surface, in neat films as well as in PM6:Y6 blends, while GIWAXS data collected at critical angles showed that the films spin-coated from CF:CN exhibited a dominant face-on orientation in the bulk for both neat PM6 films and PM6:Y6 blend films.

Pure PYT and PF5-Y5 films exhibit dichroic ratios of -0.61 and -0.58 , respectively, indicating a clear face-on orientation within the bulk of the film, and therefore a consistent face-on orientation throughout the entire film (see figures 2 and S1). The blend PBDB:PYT (1:0.75) does not show any dichroism, and the spectral shape resembles that of neat PBDB-T. However, this measurement is likely affected by experimental issues, as the spectrum recorded at 90° deviates unexpectedly from the others in the sigma region. This is not a major concern, as complementary information from the nitrogen K-edge provides reliable insight into the acceptor orientation.

The PBDB-T:PF5-Y5 (1:0.75) blend film has an average face-on orientation, with a dichroic ratio of -0.38 , extracted from the carbon K-edge spectra in FY mode, and the spectral shape still resembles mostly the PBDB-T carbon K-edge spectra, despite the bulk sensitivity. In contrast PBDB-T:PYT and PBDB-T:PF5-Y5 at 1:10 ratio show carbon K-edge spectra recorded in FY mode that closely resemble those of their respective acceptors, with dichroic ratios of -0.53 , indicating a predominant face-on molecular orientation in the bulk.

Figure S7 presents the nitrogen K-edge NEXAFS spectra recorded in FY for all samples. The dichroic ratios for neat PYT (-0.74) and PF5-Y5 (-0.68) are consistent with those from the corresponding carbon K-edge spectra, confirming a predominant face-on orientation of the pure acceptor within the bulk. The PBDB-T:PYT blend films exhibit dichroic ratios of -0.64 (1:0.75) and -0.70 (1:10), indicating that PYT retains its face-on orientation in the bulk, when blended with PBDB-T. Similarly, PBDB-T:PF5-Y5 blend films show dichroic ratios of -0.56 (1:0.75) and -0.67 (1:10), further supporting the conclusion that the acceptor maintains a face-on orientation throughout the bulk of the blend films.

Although this study does not include device measurements, the observed face-on molecular orientation is consistent with previous reports linking such arrangements to improved charge transport and higher power conversion efficiencies in non-fullerene OSCs [30]. Previous reports have shown that



face-on orientation enhance $\pi - \pi$ stacking and orbital overlap, improving electronic coupling and consequently charge transport [30, 31]. In addition, molecular orientation can influence the energy level alignment through quadrupole-induced electrostatic potential shifts, which have been linked to band bending and reduced energy offsets at donor-acceptor interfaces [16, 32]. These earlier studies highlight the importance of our findings for optimizing device efficiency.

Based on the combined results from PEY, TEY, and FY modes, figure 6 illustrates the vertical distribution of the donor PBDB-T and the acceptors (PYT or PF5-Y5) in blend films with both low and high acceptor content. The acceptor molecules are represented in red, while the donor is represented in blue, and the mixture of both is represented in purple. While NEXAFS does not provide quantitative compositional profiles, depth-dependent measurements allow qualitative assessment of vertical stratification in both blend ratios, revealing donor-enriched surfaces and consistent face-on orientation of the acceptor throughout the film. Previous studies have shown that vertical stratification is likely to occur due to phase separation driven by differences in surface energy between the polymer components in a blend film [33–37]. The component with the lowest surface energy tends to segregate towards the free surface to minimize the system's overall energy.

4. Conclusion

In this study we have demonstrated that NEXAFS spectroscopy is a valuable method to probe the molecular orientation in polymer donor: acceptor blend thin films, with particular emphasis on the selective nitrogen K-edge as a tool to distinguish acceptor orientation. The results reveal that, regardless of the co-monomer—BDT-T or thiophene—, neat films of the Y5-based acceptor polymer (PF5-Y5 and PYT) have comparable degree of face-on orientation. Depth-dependent analysis of the blend films through comparison of PEY, TEY, and FY modes revealed that PBDB-T dominates the surface composition for both blends, even at high acceptor concentrations. Nitrogen K-edge spectra confirmed that both PF5-Y5 and PYT retain their face-on orientation in blend films, consistent with their behavior in neat films. However, the difference in the dichroic ratio obtained from the nitrogen K-edge PEY spectra between the PBDB-T: PYT (1:0.75) blend (-0.43) and neat PYT (-0.77) suggests that the presence of PBDB-T slightly disrupts the acceptor's preferential face-on orientation at the film surface. In contrast, the difference observed for the PF5-Y5 blend is much smaller, indicating a weaker effect of the donor on the preferential acceptor orientation. The difference between PYT and PF5-Y5 acceptor molecules in the donor rich surface region of the blend films indicates that the nature of the co-monomer influences the acceptor's ability to maintain its face-on molecular orientation. These findings highlight the nitrogen K-edge in NEXAFS spectroscopy as a selective and sensitive probe for analyzing molecular orientation in donor-acceptor blends. This approach can be generalized to other selective edges in planar D-A systems, providing a foundation for tailoring molecular alignment to optimize the performance of all-polymer OSCs.

Data availability statement

The data cannot be made publicly available upon publication because they are not available in a format that is sufficiently accessible or reusable by other researchers. The data that support the findings of this study are available upon reasonable request from the authors.

Supplementary Data available at <http://doi.org/10.1088/2515-7639/ae409d/data1>.

Acknowledgment

We thank Robert Temperton at MAX IV Laboratory, and Hanmin Zhang and Leif Ericsson at Karlstad University for their participation in the synchrotron measurements and for fruitful discussions. We thank the FlexPES beamline team, especially Alexander Generalov and Alexei Preobrajenski, for the technical advice and assistance during the measurements at the FlexPES beamline.

E.M. acknowledges the Swedish Research Council for financial support of the project (Grant No. 2021–04798). The authors are grateful to the Knut and Alice Wallenberg Foundation (Grant Numbers 2016.0059) for the financial support of their collaborative work.

E.W. thanks the Swedish Research Council Formas (2023-01008, 2024-01110), and The Knut and Alice Wallenberg Foundation (2022.0192) and the Wallenberg Initiative Materials Science for Sustainability (WISE-AP01-D19) for financial support.

We acknowledge the MAX IV Laboratory for beamtime on the FlexPES beamline under proposal 20230295. Research conducted at MAX IV, a Swedish national user facility, is supported by Vetenskapsrådet (Swedish Research Council, VR) under contract 2018-07152, Vinnova (Swedish Governmental Agency for Innovation Systems) under contract 2018-04969, and Formas under contract 2019-02496.

ORCID iDs

Leticia P Christopholi  0009-0004-6675-4558

Zewdneh Genene  0000-0001-9776-4709

Cleber F N Marchiori  0000-0003-0377-3669

Stela Andrea Muntean  0000-0001-9337-2249

Ergang Wang  0000-0002-4942-3771

Ellen Moons  0000-0002-1609-8909

References

- [1] Chen S, Feng L, Jia T, Jing J, Hu Z, Zhang K and Huang F 2021 High-performance polymer solar cells with efficiency over 18% enabled by asymmetric side chain engineering of non-fullerene acceptors *Sci. China Chem.* **64** 1192–9
- [2] Liu K, Jiang Y, Liu F, Ran G, Huang F, Wang W, Zhang W, Zhang C, Hou J and Zhu X 2023 Organic solar cells with over 19% efficiency enabled by a 2D-conjugated non-fullerene acceptor featuring favorable electronic and aggregation structures *Adv. Mater.* **35** 2300363
- [3] Cui Y *et al* 2021 Single-junction organic photovoltaic cell with 19% efficiency *Adv. Mater.* **33** 2102420
- [4] Zhu L *et al* 2022 Single-junction organic solar cells with over 19% efficiency enabled by a refined double-fibril network morphology *Nat. Mater.* **21** 656–63
- [5] Murugan P, Hu T, Hu X and Chen Y 2022 Fused ring A–DA' D–A (Y-series) non-fullerene acceptors: recent developments and design strategies for organic photovoltaics *J. Mater. Chem. A* **10** 17968–87
- [6] Zhang Z G and Li Y 2021 Polymerized small-molecule acceptors for high-performance all-polymer solar cells *Angew. Chem., Int. Ed.* **60** 4422–33
- [7] Lee J W *et al* 2021 Efficient, thermally stable, and mechanically robust all-polymer solar cells consisting of the same benzodithiophene unit-based polymer acceptor and donor with high molecular compatibility *Adv. Energy Mater.* **11** 2003367
- [8] Fan Q *et al* 2020 Mechanically robust all-polymer solar cells from narrow band gap acceptors with hetero-bridging atoms *Joule* **4** 658–72
- [9] Zhang J *et al* 2021 π -extended conjugated polymer acceptor containing thienylene–vinylene–thienylene unit for high-performance thick-film all-polymer solar cells with superior long-term stability *Adv. Energy Mater.* **11** 2102559
- [10] Sun G *et al* 2022 High performance polymerized small molecule acceptor by synergistic optimization on π -bridge linker and side chain *Nat. Commun.* **13** 5267
- [11] Kim H K, Yu H, Pan M, Shi X, Zhao H, Qi Z, Liu W, Ma W, Yan H and Chen S 2022 Linker unit modulation of polymer acceptors enables highly efficient air-processed all-polymer solar cells *Adv. Sci.* **9** 2202223
- [12] Lee J-W, Sun C, Lee C, Tan Z, Phan T N-L, Jeon H, Jeong D, Kwon S-K, Kim Y-H and Kim B J 2023 Linker engineering of dimerized small molecule acceptors for highly efficient and stable organic solar cells *ACS Energy Lett.* **8** 1344–53
- [13] Zhou K, Wu Y, Liu Y, Zhou X, Zhang L and Ma W 2019 Molecular orientation of polymer acceptor dominates open-circuit voltage losses in all-polymer solar cells *ACS Energy Lett.* **4** 1057–64
- [14] Lee H, Lee D, Sin D H, Kim S W, Jeong M S and Cho K 2018 Effect of donor–acceptor molecular orientation on charge photogeneration in organic solar cells *NPG Asia Mater.* **10** 469–81

- [15] Zhou K, Zhang R, Liu J, Li M, Yu X, Xing R and Han Y 2015 Donor/acceptor molecular orientation-dependent photovoltaic performance in all-polymer solar cells *ACS Appl. Mater. Interfaces* **7** 25352–61
- [16] Li X E et al 2022 Mapping the energy level alignment at donor/acceptor interfaces in non-fullerene organic solar cells *Nat. Commun.* **13** 2046
- [17] Christopholi P, Marchiori C F N, Jalan I, Opitz A, Muntean S A and Moons E 2024 Role of the solvent on the orientation of Y-type acceptor molecules in spin-coated films *J. Phys. Chem. C* **128** 17825–35
- [18] Huang W, Gann E, Thomsen L, Dong C, Cheng Y-B and McNeill C R 2015 Unraveling the morphology of high efficiency polymer solar cells based on the donor polymer PBDTTT-EFT *Adv. Energy Mater.* **5** 1401259
- [19] Fan Q et al 2020 Over 14% efficiency all-polymer solar cells enabled by a low bandgap polymer acceptor with low energy loss and efficient charge separation *Energy Environ. Sci.* **13** 5017–27
- [20] Genene Z, Lee J-W, Lee S-W, Chen Q, Tan Z, Abdulahi B A, Yu D, Kim T-S, Kim B J and Wang E 2022 Polymer acceptors with flexible spacers afford efficient and mechanically robust all-polymer solar cells *Adv. Mater.* **34** 2107361
- [21] Kern W 1990 The evolution of silicon wafer cleaning technology *J. Electrochem. Soc.* **137** 1887–92
- [22] Stöhr J 2013 *NEXAFS Spectroscopy* vol. 25 (Springer Science & Business Media)
- [23] Nefedov A and Wöll C 2013 Advanced applications of nexafs spectroscopy for functionalized surfaces *Surface Science Techniques* (Springer) pp 277–303
- [24] Solé V A, Papillon E, Cotte M, Walter P and Susini J 2007 A multiplatform code for the analysis of energy-dispersive x-ray fluorescence spectra *Spectrochim. Acta B* **62** 63–68
- [25] Zheng Z, Yao H, Ye L, Xu Y, Zhang S and Hou J 2020 PBDB-T and its derivatives: a family of polymer donors enables over 17% efficiency in organic photovoltaics *Mater. Today* **35** 115–30
- [26] Rehr J J and Albers R C 2000 Theoretical approaches to x-ray absorption fine structure *Rev. Mod. Phys.* **72** 621
- [27] Zhou H, Yang L and You W 2012 Rational design of high performance conjugated polymers for organic solar cells *Macromolecules* **45** 607–32
- [28] Nahid M M, Gann E, Thomsen L and McNeill C R 2016 NEXAFS spectroscopy of conjugated polymers *Eur. Polym. J.* **81** 532–54
- [29] Neusser D et al 2022 Spectroelectrochemically determined energy levels of PM6: Y6 blends and their relevance to solar cell performance *J. Mater. Chem. C* **10** 11565–78
- [30] Wang L, Guo S, Zhou K and Ma W 2020 Control of the molecular orientation in small molecule-based organic photovoltaics *Sustain. Energy Fuels* **4** 4934–55
- [31] Li Y, Wu J, Yi X, Liu Z, Liu H, Fu Y, Liu J and Xie Z 2023 Layer-by-layer blade-coated organic solar cells with non-halogenated solvents and non-halogenated additive via adjusting morphology and crystallization *J. Mater. Chem. C* **11** 13263–73
- [32] Fu Y et al 2023 Molecular orientation-dependent energetic shifts in solution-processed non-fullerene acceptors and their impact on organic photovoltaic performance *Nat. Commun.* **14** 1870
- [33] Nilsson S, Bernasik A, Budkowski A and Moons E 2007 Morphology and phase segregation of spin-casted films of polyfluorene/P-CBM blends *Macromolecules* **40** 8291–301
- [34] Jones R A, Norton L J, Kramer E J, Bates F S and Wiltzius P 1991 Surface-directed spinodal decomposition *Phys. Rev. Lett.* **66** 1326
- [35] Chen Z, Zhang S, Ren J, Zhang T, Dai J, Wang J, Ma L, Qiao J, Hao X and Hou J 2024 Molecular design for vertical phase distribution modulation in high-performance organic solar cells *Adv. Mater.* **36** 2310390
- [36] Zhang X et al 2022 Systematically controlling acceptor fluorination optimizes hierarchical morphology, vertical phase separation, and efficiency in non-fullerene organic solar cells *Adv. Energy Mater.* **12** 2102172
- [37] Anselmo A S, Lindgren L, Rysz J, Bernasik A, Budkowski A, Andersson M R, Svensson K, van Stam J and Moons E 2011 Tuning the vertical phase separation in polyfluorene: fullerene blend films by polymer functionalization *Chem. Mater.* **23** 2295–302